Electronic Supplementary Material (ESI) for Inorganic Chemistry Frontiers.

Supplementary Information

Effect of -OH on the Thermal Enhancement Properties of NIR-II Lanthanide Doped Nanoparticles in Water

Yingping Huang[a,b,c], *Jie Hu*[a,b,c,*] *Yongwei Guo*[a,c], *Zihao Wang*[a,c], *Fulin Lin*[a,c], *Haomiao Zhu*[a,b,c,*]

[a] CAS Key Laboratory of Design and Assembly of Functional Nanostructures, and Fujian Key Laboratory of Nanomaterials, Fujian Institute of Research on the Structure of Matter, Chinese Academy of Sciences, Fuzhou 350002, China

[b] Fujian Provincial Key Laboratory of Polymer Materials, College of Chemistry and Materials Science, Fujian Normal University, Fuzhou 350007, China

[c] Xiamen Key Laboratory of Rare Earth Photoelectric Functional Materials, Xiamen Institute of Rare Earth Materials, Haixi Institutes, Chinese Academy of Sciences, Xiamen, Fujian 361021, China

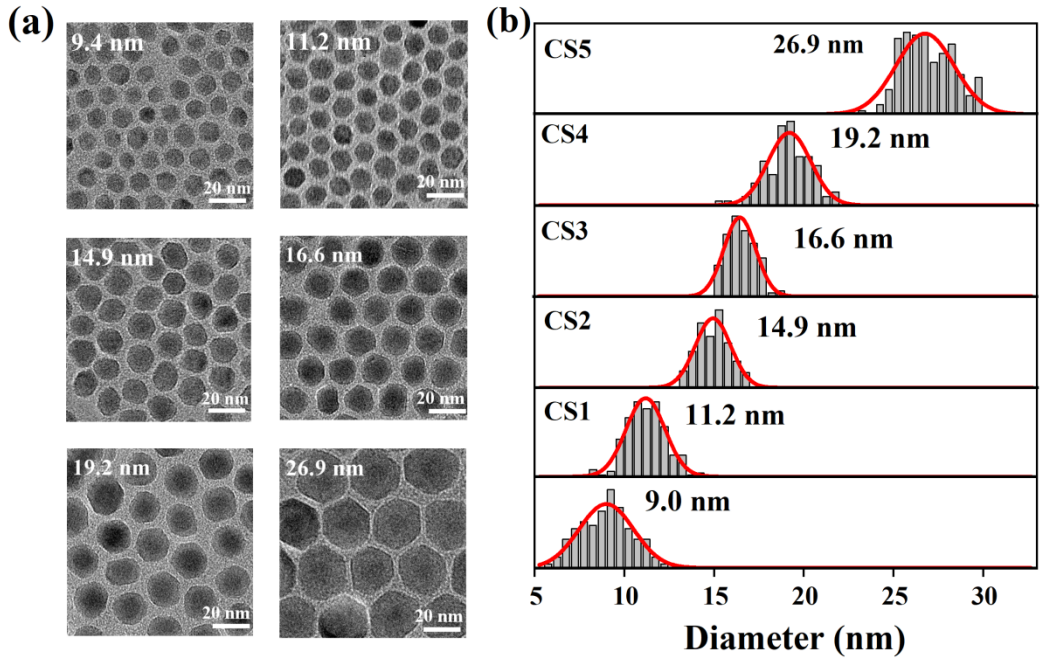

Figure S1 (a) TEM images and **(b)** size distribution of the as-prepared α-$NaYbF_4$: 2%Er, 2%Ce core NPs and α-$NaYbF_4$: 2%Er, 2%Ce@$NaYF_4$ core-shell NPs.

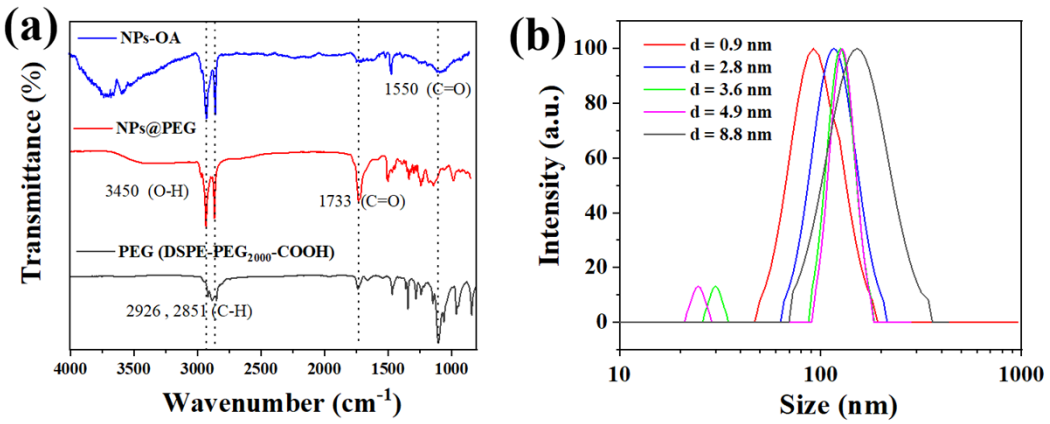

Figure S2 (a) FTIR measurements of the α-$NaYbF_4$: 2%Er, 2%Ce@$NaYF_4$ core-shell NPs capped with oleic acid (OA) and DSPE-PEG_{2000}-COOH, and only DSPE-PEG_{2000}-COOH. **(b)** Dynamic light scattering (DLS) measurements of NPs@PEG with different shell thicknesses (d = 0.9, 2.8, 3.6, 4.9, and 8.8 nm).

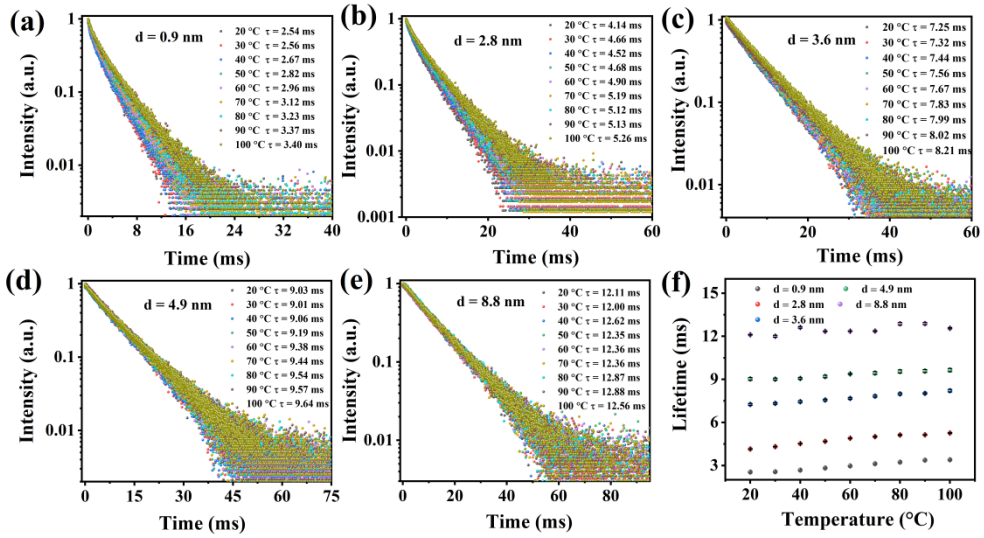

Figure S3 (a-e) Temperature dependent PL decay curves of NPs with different shell thickness (d = 0.9, 2.8, 3.6, 4.9, and 8.8 nm) monitored at 1532 nm under excitation at 980 nm. (f) Corresponding PL lifetime of (a-e) samples as a function of temperature.

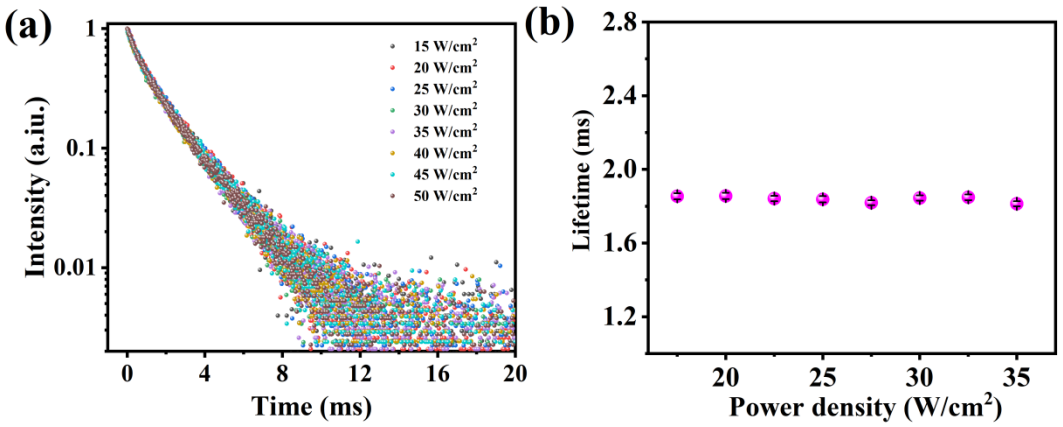

Figure S4 (a) PL decay curves of NPs@PEG (d = 3.6 nm) dispersed in aqueous solution monitored at 1532 nm under excitation at 980 nm with different excitation power density. (b) Corresponding PL lifetime of NPs@PEG (d = 3.6 nm) as a function of excitation power density.

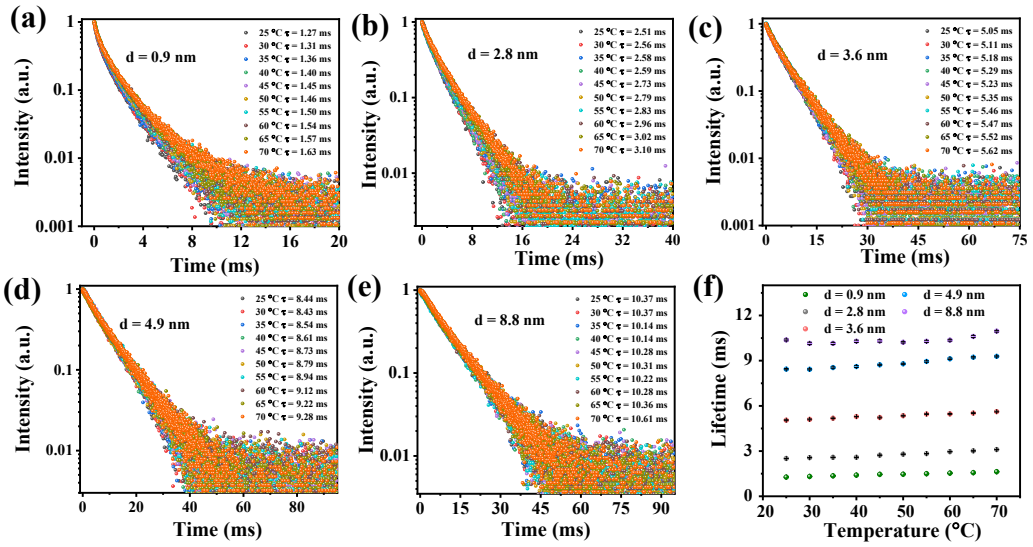

Figure S5 (a-e) Temperature dependent PL decay curves of NPs@PEG with different shell thicknesses (d = 0.9, 2.8, 3.6, 4.9, and 8.8 nm) dispersed in aqueous solution monitored at 1532 nm under excitation at 980 nm. (f) Corresponding PL lifetime of (a-e) samples as a function of temperature.

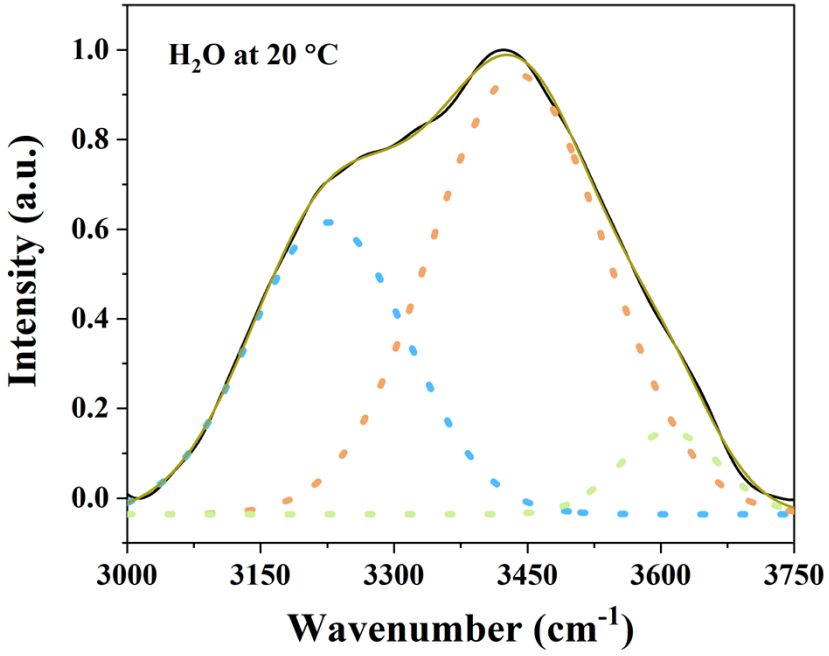

Figure S6 The Raman spectra of H_2O from 3000 cm^{-1} to 3750 cm^{-1}, and the gaussian fitting of H_2O at 20 °C shows the stretching of −OH band can be divided into three components, 3226 cm^{-1}, 3439 cm^{-1} and 3610 cm^{-1}.

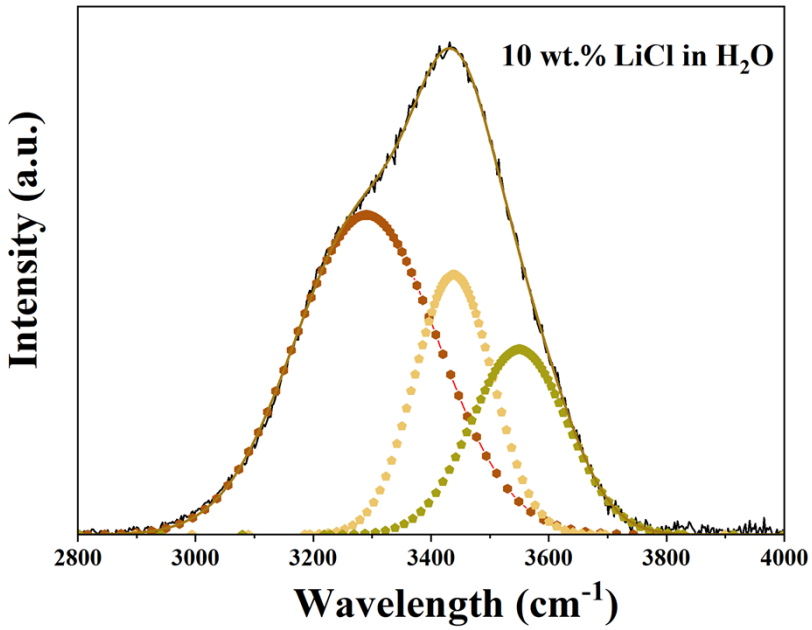

Figure S7 The Raman spectra of 10 wt.% LiCl solution from 2800 cm^{-1} to 4000 cm^{-1}, and the gaussian fitting of 10 wt.% LiCl solution shows the stretching of −OH band can be divided into three components, 3226 cm^{-1}, 3439 cm^{-1} and 3610 cm^{-1}.

Table S1 The gaussian fitting parameters (area of components and R^2) of temperature dependent Raman spectra of NPs@PEG (d = 3.6 nm) in aqueous solution.

Area	20 °C	30 °C	40 °C	50 °C	60 °C	70 °C
3226 cm^{-1}	144.6	124.7	95.0	44.2	36.4	35.1
3439 cm^{-1}	241.8	254.9	265.2	245.8	250.3	257.3
3610 cm^{-1}	26.0	17.6	10.5	3.5	5.4	9.6
COD (R^2)	0.9995	0.9996	0.9993	0.9943	0.9934	0.9942

Table S2 The gaussian fitting parameters (area of components and R^2) of Raman spectra of NPs@PEG (d = 3.6 nm) in LiCl solution.

Area	0 wt.%	5 wt.%	10 wt.%	20 wt.%	30 wt.%
3226 cm^{-1}	185.1	113.0	103.2	87.6	63.8
3439 cm^{-1}	212.5	234.0	240.4	226.0	231.6
3610 cm^{-1}	21.2	12.4	11.8	14.3	8.0
COD (R^2)	0.9983	0.9986	0.9989	0.9964	0.9983

Table S3 The gaussian fitting parameters (area of components and R^2) of temperature dependent Raman spectra of NPs@PEG (d = 3.6 nm) in 10 wt.% LiCl solution.

Area	20 °C	30 °C	40 °C	50 °C	60 °C	70 °C
3226 cm^{-1}	114.0	112.8	97.2	89.5	82.6	75.0
3439 cm^{-1}	239.7	241.1	245.5	236.2	236.7	237.2
3610 cm^{-1}	11.3	13.4	9.2	23.1	17.3	12.8
COD (R^2)	0.9987	0.9988	0.9983	0.9970	0.9968	0.9961

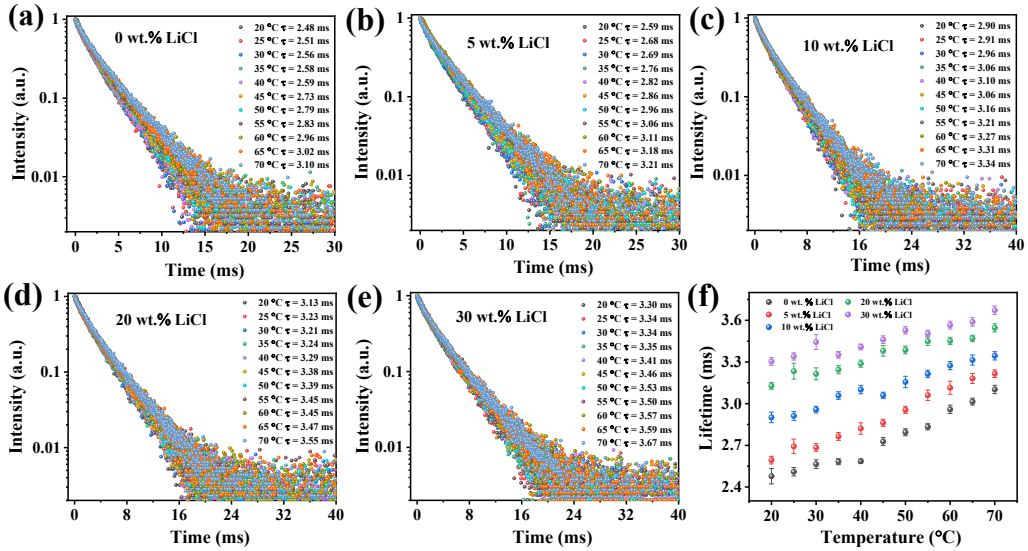

Figure S8 (a-e) Temperature dependent PL decay curves of NPs@PEG (d = 3.6 nm) dispersed in different concentrations of LiCl solution monitored at 1532 nm under excitation at 980 nm. (f) Corresponding PL lifetime of (a-e) samples as a function of temperature.

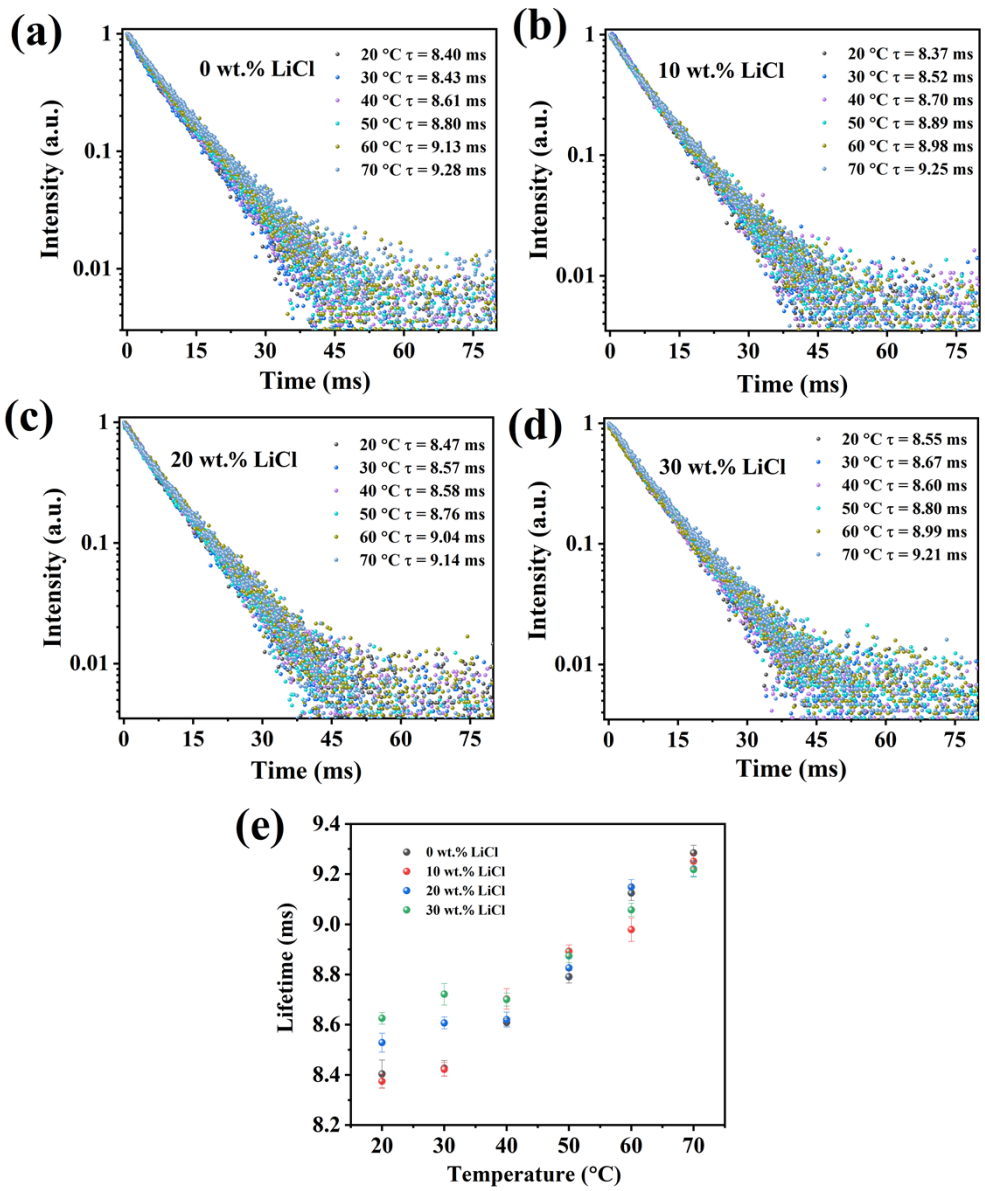

Figure S9 (a-d) Temperature dependent PL decay curves of NPs@PEG (d = 8.8 nm) dispersed in different concentrations of LiCl solution monitored at 1532 nm under excitation at 980 nm. (e) Corresponding PL lifetime of (a-d) samples as a function of temperature.

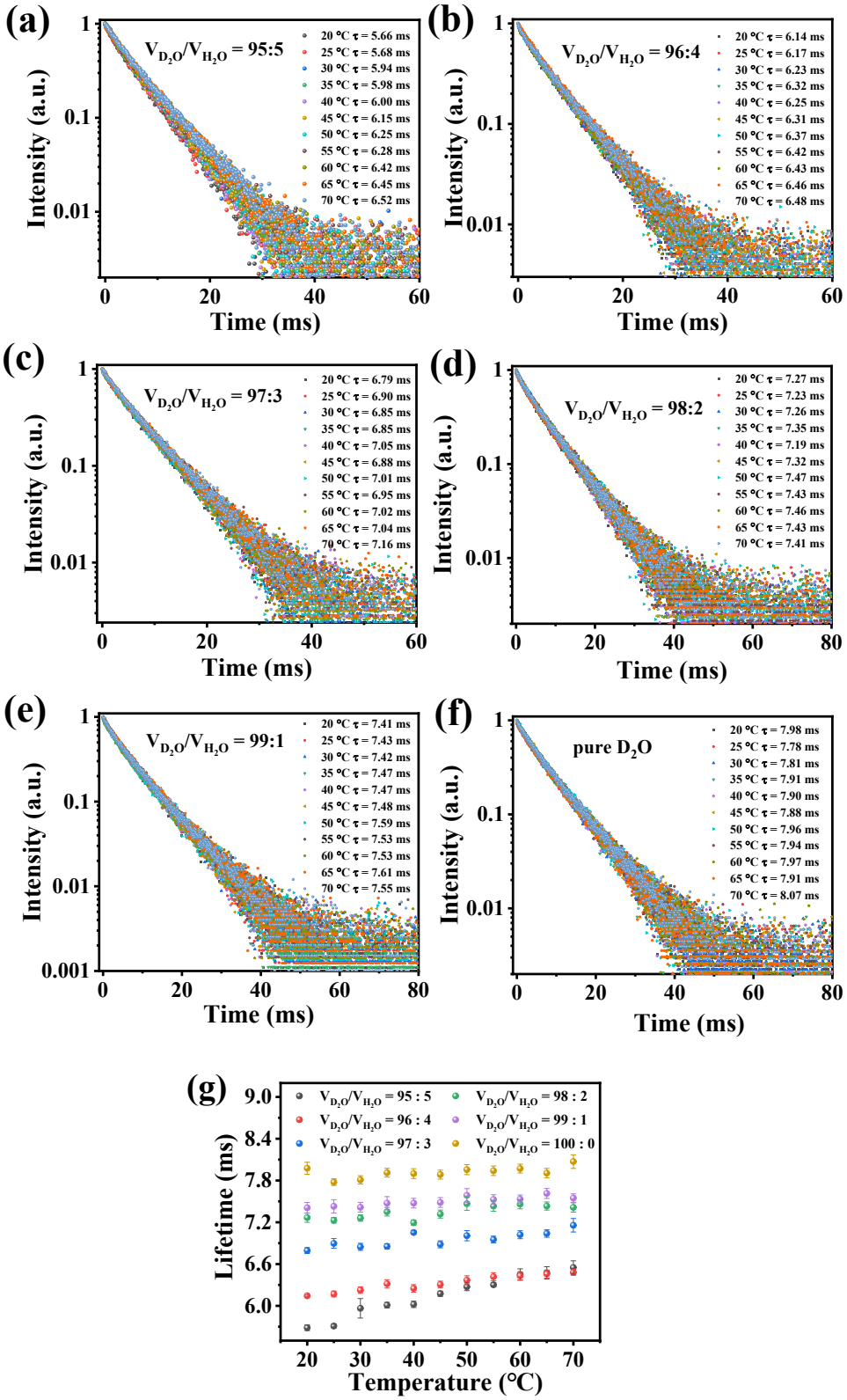

Figure S10 (a-f) Temperature dependent PL decay curves of NPs@PEG (d = 3.6 nm) dispersed in different ratio of V_{D_2O}/V_{H_2O} monitored at 1532 nm under excitation at 980 nm. (g) Corresponding PL lifetime of (a-f) samples as a function of temperature.

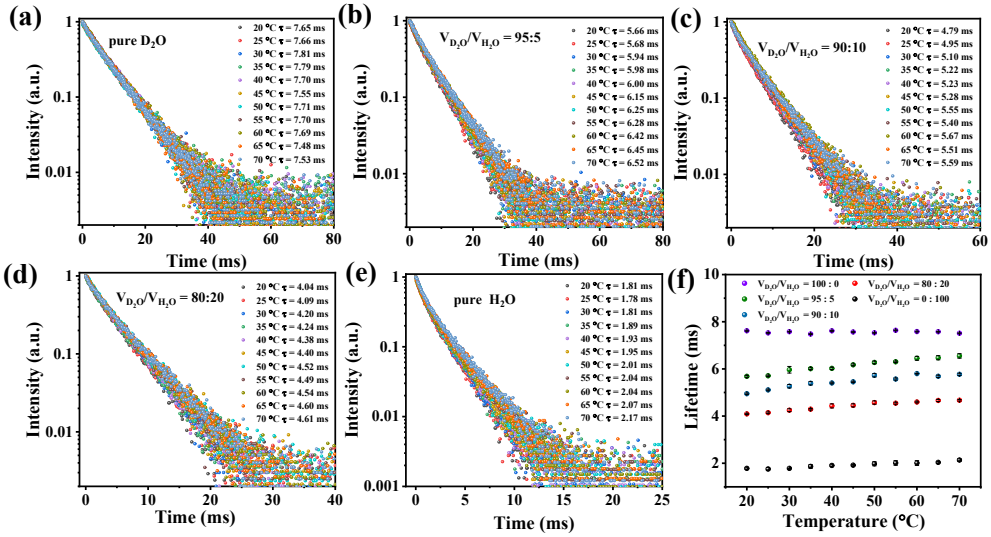

Figure S11(a-e) Temperature dependent PL decay curves of NPs@PEG (d = 3.6 nm) dispersed in different ratio of V_{D_2O}/V_{H_2O} (change in large scale) monitored at 1532 nm under excitation at 980 nm. (f) Corresponding PL lifetime of (a-e) samples as a function of temperature.

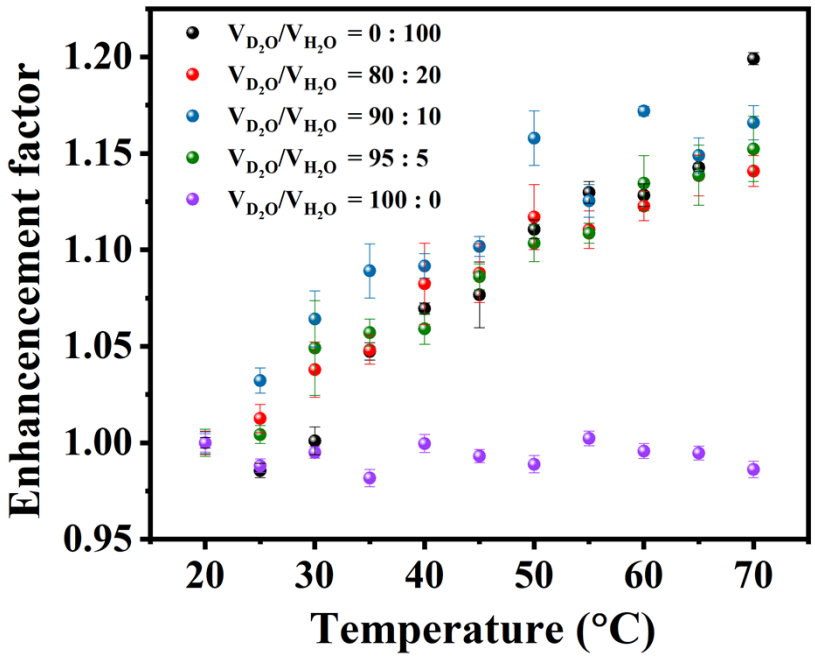

Figure S12 Temperature dependent thermal enhancement factor of NPs@PEG (d = 3.6 nm) dispersed in different ratio of V_{D_2O}/V_{H_2O} monitored at 1532 nm under excitation at 980 nm.